iScience

CellPress
OPEN ACCESS

Article

Decomposing loss aversion from a single neural signal

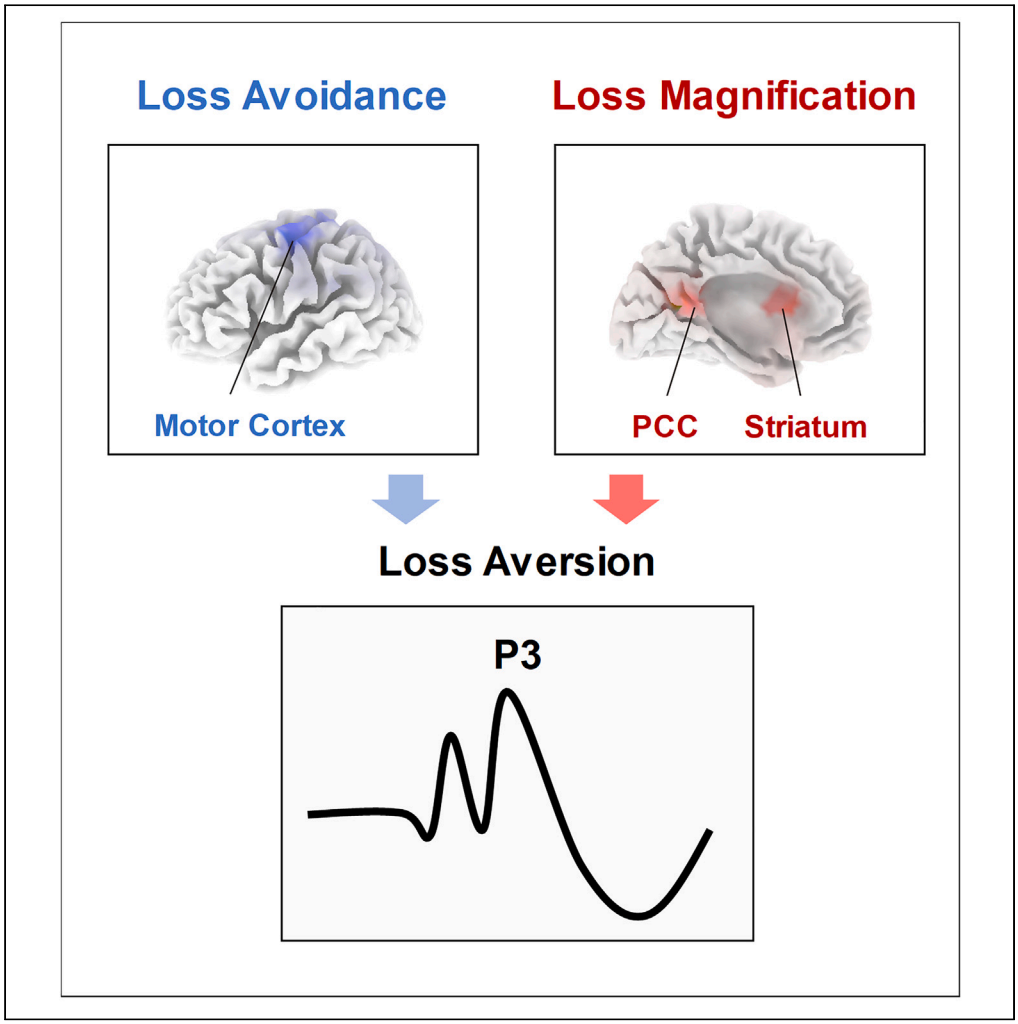

Ruining Wang, Xiaoyi Wang, Michael L. Platt, Feng Sheng

fsheng@zju.edu.cn

Highlights

Loss aversion can be decomposed into valuation bias and response bias

Valuation bias manifests as larger sensitivity of P3 to losses than gains

Response bias manifests as larger P3 preceding choices that may incur losses

Distinct types of loss-averse decision makers can be identified based on P3 activity

Wang et al., iScience 27, 110153
July 19, 2024
https://doi.org/10.1016/j.isci.2024.110153

iScience

CellPress
OPEN ACCESS

Article

Decomposing loss aversion from a single neural signal

Ruining Wang,[1,2,3,4] Xiaoyi Wang,[1,2,3,4] Michael L. Platt,[5,6,7,8] and Feng Sheng[1,2,3,4,5,9,10,*]

SUMMARY

People often display stronger aversion to losses than appetite for equivalent gains, a widespread phenomenon known as loss aversion. The prevailing theory attributes loss aversion to a valuation bias that amplifies losses relative to gains. An alternative account attributes loss aversion to a response bias that avoids choices that might result in loss. By modeling the temporal dynamics of scalp electrical activity during decisions to accept or reject gambles within a sequential sampling framework, we decomposed valuation bias and response bias from a single event-related neural signal, the P3. Specifically, we found valuation bias manifested as larger sensitivity of P3 to losses than gains, which was localizable to reward-related brain regions. By contrast, response bias manifested as larger P3 preceding gamble acceptance than rejection and was localizable to motor cortex. Our study reveals the dissociable neural biomarkers of response bias and valuation bias underpinning loss-averse decisions.

INTRODUCTION

Risky decisions often involve the prospect of gaining and the possibility of losing. Relative to the appetite for potential gains, people typically exhibit a stronger degree of aversion to equivalent losses, a widespread phenomenon known as loss aversion.[1] For example, people often reject gambles of equal odds to win and lose money, so-called mixed gambles, even when the potential gain is larger than the potential loss.[2] Loss aversion has been widely observed in both laboratory studies[1–4] and field studies,[5–7] is evident in both human and non-human primates,[8,9] and has been linked to a variety of psychiatric conditions such as depression,[10,11] anxiety,[12,13] schizophrenia,[14,15] and obsessive-compulsive disorder.[16]

Despite the prevalence of loss aversion, its underlying mechanism remains controversial. Conventionally, loss aversion has been attributed to a valuation bias of amplifying potential losses over potential gains.[1] Accordingly, people would reject a mixed gamble unless there is a larger potential gain that could counteract the impact of asymmetric weighting. Alternatively, loss aversion has been attributed to a response bias to avoid an option that may incur losses relative to the status quo, or the so-called status quo bias.[17–20] Accordingly, people would reject a gamble that may cause losses, unless there is an extra gain that could motivate them to overcome their inertia. Thus, loss aversion can be explained either by valuation bias or by response bias.[21]

Distinct neural systems have been linked to loss aversion in prior research. An influential functional magnetic resonance imaging (fMRI) study[4] showed that the prefrontal-striatal dopaminergic system displays larger sensitivity to the magnitude of losses than to the magnitude of gains, which may reflect valuation bias. By contrast, activity in the noradrenergic arousal system, which is implicated in stress response to threats,[22] has been linked to loss aversion by studies using positron emission tomography (PET),[23] pharmacological manipulations,[24] psychophysiological responses,[25] and observation of decision-making in patients with brain damage.[3] Thus, both the valuation-bias account and the response-bias account find support in a disparate array of neurobiological studies.

Decision-making is not instantaneous but is often a process of evidence accumulation over time that culminates in a response,[26] which can be formally described by sequential sampling models such as the drift diffusion model (DDM).[27] By unfolding the decision to accept or reject a mixed gamble as an evidence accumulation process, we recently integrated valuation bias and response bias in a unified computational model.[28] Specifically, we theorized that valuation bias would modulate how gains and losses were evaluated during evidence accumulation, and response bias would modulate how much evidence needs to be accumulated, to choose whether or not to accept a gamble. By coupling this model with eye-tracking and pupillometry, we showed that valuation bias of magnifying losses was associated with

[1]School of Management, Zhejiang University, Hangzhou, Zhejiang 310058, China
[2]State Key Lab of Brain-Machine Intelligence, Zhejiang University, Hangzhou, Zhejiang 310058, China
[3]MOE Frontier Science Center for Brain Science & Brain-Machine Integration, Zhejiang University, Hangzhou, Zhejiang 310058, China
[4]Neuromanagement Laboratory, Zhejiang University, Hangzhou, Zhejiang 310058, China
[5]Wharton Neuroscience Initiative, the Wharton School, University of Pennsylvania, Philadelphia, PA 19104, USA
[6]Department of Neuroscience, Perelman School of Medicine, University of Pennsylvania, Philadelphia, PA 19104, USA
[7]Department of Psychology, University of Pennsylvania, Philadelphia, PA 19104, USA
[8]Marketing Department, the Wharton School, University of Pennsylvania, Philadelphia, PA 19104, USA
[9]Senior author
[10]Lead contact
*Correspondence: fsheng@zju.edu.cn
https://doi.org/10.1016/j.isci.2024.110153

preferential attention to losses, which was indexed by biased gaze allocation.[29] By contrast, response bias to avoid losses was observed in larger physiological arousal when accepting relative to rejecting gambles, which was indexed by pupil dilation.[30] Our approach integrates the two competing accounts of loss aversion within a single evidence-accumulation model. However, to date, no direct neural evidence has been provided for this two-dimensional framework. Here, we seek to fill this gap by exploiting scalp electrophysiological activity, which can be measured noninvasively using electroencephalography (EEG). We focus on the event-related potential (ERP) P3 or P300—a positive deflection in the EEG signal that peaks about 300–500 ms after stimulus onset and is observed in a variety of decision tasks.[31–33] P3 is probably the most intensively studied ERP and has been hypothesized to reflect the ongoing updating of mental representations in response to incoming information.[31] In other words, changes in the amplitude of P3 reflect the extent to which a mental representation is updated. Notably, this classic hypothesis of P3[34] can also accommodate the recent study linking P3 to evidence-accumulation during decision-making.[35] That is, P3 may reflect the dynamics of mental representations that are continuously updated as evidence is accumulated during the decision process.

Accordingly, we hypothesize that response bias and valuation bias in loss-averse decisions should both be reflected in P3. Specifically, in decisions involving mixed-gambles, a response bias to avoid losses should manifest as a larger P3 when accepting compared to rejecting a gamble, because accepting a gamble requires more evidence to be accumulated than rejecting it. A valuation bias that magnifies losses should manifest as larger sensitivity of P3 to potential losses than to potential gains, because information about losses provides stronger evidence than information about an equivalent amount of gains during the decision process.

To test these hypotheses, we recorded EEG from participants ($N = 41$) making decisions to accept or reject mixed gambles of equal odds to win and lose money (Figure 1A, see STAR Methods for details). We simultaneously modeled their choices and reaction times to decompose decisions into valuation bias and response bias using DDM. We then deconstructed P3 signals into P3 response differential, which quantified the difference in P3 amplitudes for gamble acceptance vs. rejection, and P3 valuation differential, which quantified the difference in P3 responses to large vs. small amounts of gains vs. losses. We hypothesized that P3 response differential would be correlated with response bias but not valuation bias, and P3 valuation differential would be correlated with valuation bias but not response bias. We further hypothesized the P3 response differential, and the P3 valuation differential would be underpinned by distinct brain regions that could be identified by source localization. By doing so, we aimed to reveal dissociable biomarkers of response bias and valuation bias multiplexed within a single electrophysiological signal.

RESULTS

Loss aversion was observed in both choices and response times

We first analyzed participants' choices and response times in the mixed-gamble task. Despite the symmetric design of the gamble set, participants accepted fewer than half of all gambles (Figure 1B, M ± SD = 26.8 ± 9.7%, t(40) = −15.276, $p < 0.001$) and demanded a premium to be indifferent to accepting and rejecting gambles (i.e., the expected value entailing 50% probability of acceptance, Figure S1A, M ± SD = ¥ 15.579 ± 7.854, t(40) = 12.701, $p < 0.001$). They were also slower to accept (Figure 1C, M ± SD = 1.733 ± 0.567) than reject gambles (M ± SD = 1.212 ± 0.395, t(40) = −7.138, $p < 0.001$, Cohen's $d = 1.115$) and took the longest time to accept gambles with a premium larger than zero (i.e., the expected value entailing the largest response time, Figure S1B, M ± SD = ¥ 16.951 ± 20.245, t(40) = 5.361, $p < 0.001$).

Computational modeling dissociated response bias and valuation bias

We next applied the DDM we constructed previously[28] to provide a simultaneous account for observed choices and response times. In this model, we assumed the decision to accept or reject a gamble as the outcome of a noisy evidence accumulation process drifting between two response boundaries (Figure 1D). The gamble is accepted when the process reaches the upper boundary (denoted by 1) and rejected when it reaches the bottom boundary (denoted by 0). The speed with which evidence is accumulated, or drift rate, v, is determined by the linear combination of weighted gain and loss, i.e., $v \sim v_G \cdot G - v_L \cdot L$, where G and L denote the magnitudes of potential gains and losses and v_G and v_L denote the assigned weights, respectively. We quantified valuation bias as the log-transformed ratio of the two weights, $\ln(v_L/v_G)$, which is greater than 0 when losses are overweighed. The starting point of the evidence accumulation process, z, determines initial inclination toward one of the two boundaries. We quantified response bias as the deviance of the starting point from the middle point, 0.5-z, which is greater than 0 when there is an inclination toward rejecting gambles. Critically, in this model, either a valuation bias amplifying potential losses [i.e., $\ln(v_L/v_G) > 0$] or a response bias favoring gamble rejection (i.e., $0.5\text{-}z > 0$) would yield a larger probability and a faster speed to reject compared to accept a gamble. By fitting this model simultaneously to choices and response times, we were able to identify valuation bias and response bias for each participant (Figure 1E). See STAR Methods for details.

Overall, we found both response bias favoring gamble rejection (M ± SD = 0.099 ± 0.081, t(40) = 7.858, $p < 0.001$) and valuation bias amplifying potential losses (M ± SD = 0.874 ± 0.647, t(40) = 8.642, $p < 0.001$), with a moderate correlation between the two biases ($r = 0.369$, $p = 0.018$), as observed in our prior study.[28] To test the independence of the two biases, we compared this model, denoted as DDM4, against three reduced models, namely, DDM3, which zeroed out valuation bias (i.e., $v_G = v_L$), DDM2, which zeroed out response bias (i.e., $z = 0.5$), and DDM1, which constrained both biases (i.e., $z = 0.5$, $v_G = v_L$). We found the full model, which allowed both valuation bias and response bias to vary freely, performed the best (DIC: DDM4, 12350; DDM3, 13096; DDM2, 13486; DDM1, 14289). Thus, both response bias and valuation bias were necessary to account for the observed choices and response times in our sample.

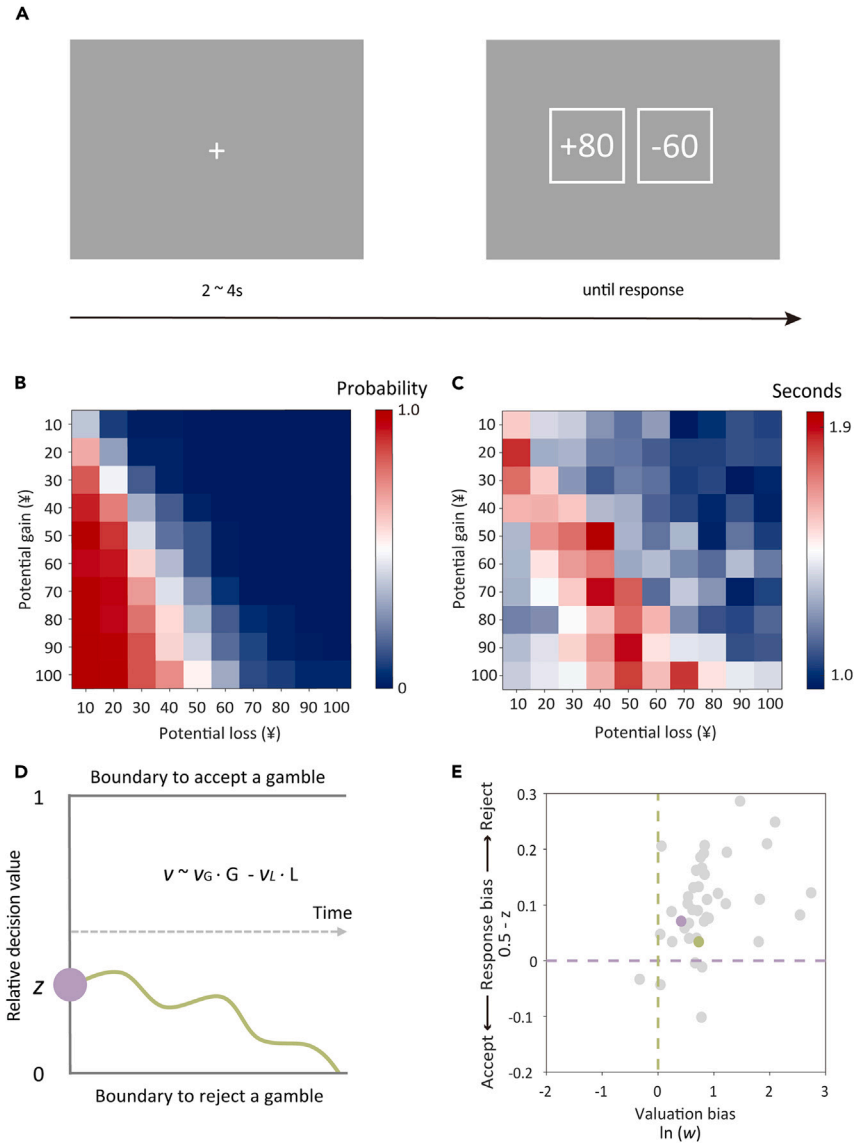

Figure 1. Task and behavior

(A) An illustration of the mixed-gamble task.

(B) Probability of gamble acceptance across gambles.

(C) Response times across gambles.

(D) An illustration of the DDM. See STAR Methods for model specifications.

(E) Valuation bias and response bias computed from DDM. Every point denotes a participant. The purple (P14) and green (P22) dots represent the two example participants described in the text (Figures 5 and 6).

Response bias manifested as a larger P3 for gamble acceptance than rejection

We next examined the ERPs accompanying the decision process with a focus on P3. As expected, we found a typical P3 that emerged approximately 300 ms after gamble onset, peaked around 450 ms, and declined slowly until about 800 ms, with a larger amplitude at the parietal site Pz than the frontal site Fz (Figure S2). We calculated the mean amplitude of P3 within the 400–700 ms window for each trial and then computed the average across trials for each participant separately for accept and reject choices.

As predicted, we found P3 was significantly larger when gambles were accepted than rejected, at both the frontal site (Figures 2A and 2B, $\Delta M \pm SD = 3.155 \pm 4.402$, $t(40) = 4.589$, $p < 0.001$, Cohen's $d = 0.717$) and parietal site (Figures S3A and S3B, $\Delta M \pm SD = 1.294 \pm 2.198$, $t(40) = 3.769$, $p < 0.001$, Cohen's $d = 0.589$). We then calculated what we termed *P3 response differential* for each participant as the difference of P3 amplitude in response to gamble acceptance versus rejection, i.e., P3accept−P3reject. While the P3 amplitude was larger at the parietal

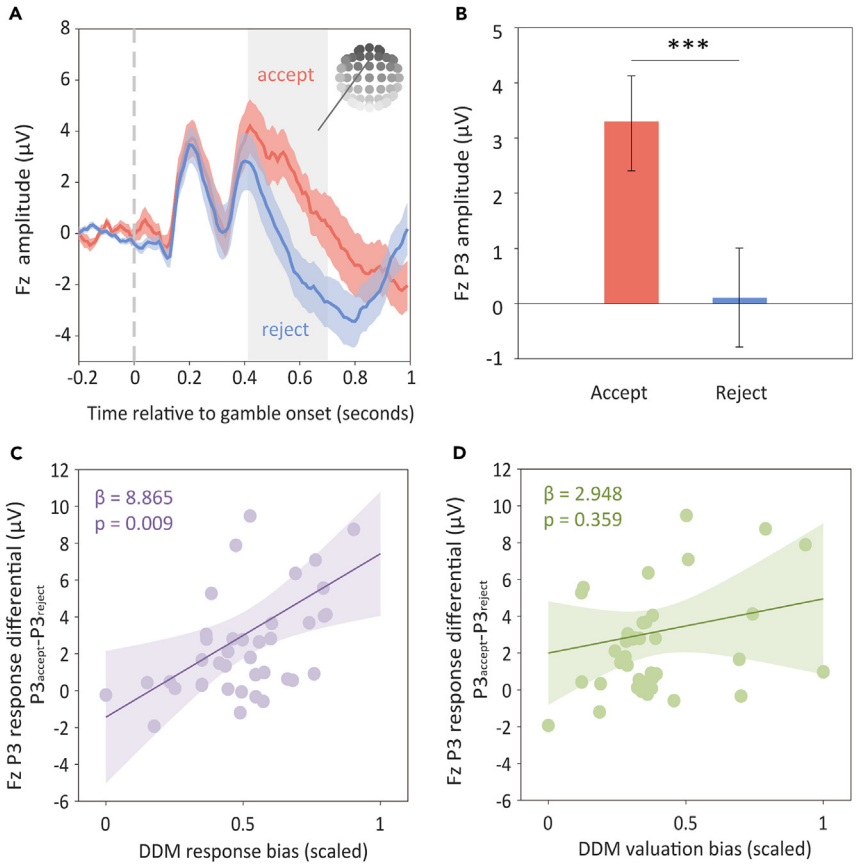

Figure 2. Frontal electrophysiological responses to gamble acceptance and rejection

(A) The mean amplitudes of ERPs locked to the onsets of gambles that were accepted (red) and rejected (blue), respectively. Shaded areas indicate ±SEM. The gray rectangle indicates the temporal window of analysis. The topography at the top-right corner indicates P3 response differential across electrodes, with the darker gray representing larger values.

(B) Mean P3 amplitudes for accepted and rejected gambles. Error bars indicate ±SEM. ***$p < 0.001$; ns: non-significant, $p > 0.1$.

(C and D) Relationships between P3 response differential and the two DDM biases. The purple (C) and green (D) lines were fitted with a regression simultaneously on DDM response bias and valuation bias that rescaled to values between 0 and 1.

site than the frontal site (Figure S2), the P3 response differential was larger at the frontal site (Figure S4, ΔM ± SD = 1.861 ± 2.875, t(40) = 4.145, $p < 0.001$, Cohen's $d = 0.647$; also see the topography at the top-right corner of Figure 2A). This is consistent with a recent report showing the special role of frontal but not parietal scalp electrical activity in value-based decision-making.[36]

We then tested whether P3 response differential was associated with the behavioral response bias identified from DDM. To do this, we regressed the P3 response differential on response bias across participants, with valuation bias included as a control variable. At the frontal site, P3 response differential was predicted by response bias (Figure 2C, Beta = 8.865, SE = 3.208, 95% confidence interval [CI]: 2.371 to 15.359, $p = 0.009$) but not by valuation bias (Figure 2D, Beta = 2.948, SE = 3.177, 95% CI: −3.483 to 9.379, $p = 0.359$); the predictive power of response bias was 3.01 times larger than that of valuation bias. At parietal site, P3 response differential was again associated with response bias (Figure S3C, Beta = 3.621, SE = 1.598, 95% CI: 0.386 to 6.857, $p = 0.029$) but not valuation bias (Figure S3D, Beta = 2.606, SE = 1.583, 95% CI: −0.598 to 5.809, $p = 0.108$); the predictive power of response bias was 1.39 times larger than that of valuation bias.

Together, these findings endorse the hypothesis that the differential P3 amplitude preceding choices reflects the different amounts of evidence required to accept versus reject gambles. Notably, this relationship is more prominent over the frontal lobe than the parietal lobe. Thus, frontal P3 response differential can be considered a neural biomarker of response bias.

Valuation bias manifested as larger sensitivity of P3 to losses than gains

We next asked whether the P3 manifests differently to the magnitude of potential gains and losses. To test the sensitivity of P3 to the magnitude of potential gains, we half split all gambles into low-gain (≤¥50) and high-gain (>¥50) gambles and, for each participant, calculated the mean P3 within the 400–700 ms window for each half of gambles. Similarly, to test the responsiveness of P3 to the amplitude of potential losses, we half split all gambles into low-loss (≤¥50) and high-loss (>¥50) gambles and, for each participant, computed the mean P3 within

the 400–700 ms window for each half of gambles. Because our gamble set was designed to be symmetric, with both gains and losses ranging from ¥10 to ¥100 (Figures 1B and 1C), the overall monetary difference between high-gain and low-gain gambles and that between low-loss and high-loss gambles were the same. Consequently, if P3 was equally sensitive to the magnitude of gains and that of losses, we would expect the differential P3 between high-gain and low-gain gambles to be equal to the differential P3 between low-loss and high-loss gambles.

We found low-loss gambles evoked a larger frontal P3 than high-loss gambles (Figures 3A and 3C, $\Delta M \pm SD = 1.504 \pm 2.447$, $t(40) = 3.937$, $p < 0.001$, Cohen's $d = 0.615$), and conversely, high-gain gambles evoked a larger frontal P3 than low-gain gambles (Figures 3B and 3C, $\Delta M \pm SD = 0.682 \pm 1.766$, $t(40) = 2.474$, $p = 0.018$, Cohen's $d = 0.386$). This opposite pattern for gains and losses in the frontal P3 in response to the magnitude of gains and losses is consistent with the larger frontal P3 for gamble acceptance vs. rejection. That is, either a small potential loss or a large potential gain leads to both gamble acceptance and high P3 amplitude.

Importantly, the sensitivity of the frontal P3 to gains and losses was asymmetric. We found a greater difference in frontal P3 for low-loss vs. high-loss gambles compared to high-gain vs. low-gain gambles (Figure 3C, $\Delta M \pm SD = 0.822 \pm 2.377$, $t(40) = 2.214$, $p = 0.033$, Cohen's $d = 0.346$), demonstrating larger sensitivity of P3 to losses than gains. To confirm this finding, we performed a more rigorous analysis by regressing the amplitudes of frontal P3 simultaneously on the magnitudes of gains and losses in a multi-level model. We found the decrease of frontal P3 by unit loss (Figure 3D, Beta = −2.667, SE = 0.574, 95% CI: −3.792 to −1.542, $p < 0.001$) was 2.120 times larger than the increase by unit gain (Beta = 1.258, SE = 0.548, 95% CI: 0.183 to 2.332, $p = 0.022$; linear contrast of Betas, $F(1,8197) = 4.006$, $p = 0.045$).

To examine whether the differential sensitivity of the frontal P3 to the magnitude of potential gains and losses reflects valuation bias, for each participant, we calculated what we termed *P3 valuation differential* as the difference in the differential P3 amplitude for low-loss vs. high-loss gambles and that for high-gain vs. low-gain gambles, i.e., $(P3_{low\text{-}loss} - P3_{high\text{-}loss}) - (P3_{high\text{-}gain} - P3_{low\text{-}gain})$. We then regressed frontal P3 valuation differential on behavioral valuation bias across participants and controlled for response bias. We found that individual differences in frontal P3 valuation differential was predicted by behavioral valuation bias (Figure 3F, Beta = 3.905, SE = 1.812, 95% CI: 0.236 to 7.574, $p = 0.038$) but not behavioral response bias (Figure 3E, Beta = 1.053, SE = 1.830, 95% CI: −2.653 to 4.758, $p = 0.569$). The predictive power of valuation bias was 3.71 times larger than response bias. This result confirms a selective relationship between P3 valuation differential and behavioral valuation bias.

We calculated parietal P3 valuation differential in the same way for each participant. The mean P3 valuation differential over parietal cortex was significantly smaller than that over frontal cortex (Figure S6, $\Delta M \pm SD = -0.799 \pm 1.830$, $t(40) = -2.795$, $p = 0.008$, Cohen's $d = 0.437$; also see the topography at the top-right corner of Figure 3A). Although parietal P3 also differentiated the magnitudes of losses (Figures S5A and S5C, low vs. high, $\Delta M \pm SD = 0.452 \pm 1.152$, $t(40) = 2.515$, $p = 0.016$, Cohen's $d = 0.393$) and gains (Figures S5B and S5C, high, vs. low, $\Delta M \pm SD = 0.429 \pm 1.040$, $t(40) = 2.640$, $p = 0.012$, Cohen's $d = 0.412$), the magnitude effects were symmetric (Figure S5C, $\Delta M \pm SD = 0.023 \pm 1.405$, $t(40) = 0.106$, $p = 0.916$, Cohen's $d = 0.017$). Multilevel regression analysis confirmed that the change of parietal P3 amplitude was similar in response to either the decrease of a unit loss (Figure S5D, Beta = −0.787, SE = 0.296, 95% CI: −1.367 to −0.205, $p = 0.008$) or the increase of a unit gain (Beta = 0.882, SE = 0.281, 95% CI: 0.331 to 1.434, $p = 0.002$; linear contrast of Betas, $F(1,8197) = 0.058$, $p = 0.810$). Further, the parietal P3 valuation differential was predicted neither by behavioral valuation bias (Figure S5F, Beta = 1.374, SE = 1.141, 95% CI: −0.937 to 3.684, $p = 0.236$) nor behavioral response bias (Figure S5E, Beta = −0.707, SE = 1.153, 95% CI: −3.040 to 1.626, $p = 0.543$).

Together, these findings indicate that the behavioral valuation bias to amplify potential losses was selectively indexed by frontal but not parietal P3 response to potential losses versus potential gains. The frontal P3 valuation differential can thus be considered a neural biomarker of behavioral valuation bias.

P3 response differential and valuation differential originated from distinct neural systems

Our findings uncovered a double dissociation in which P3 response differential selectively indexed response bias, whereas P3 valuation differential selectively indexed valuation bias. This double dissociation invites the possibility that the two P3 differentials arise from neural activity in distinct brain regions. To test this hypothesis, we modeled the sources of electrical currents within the brain that were most likely to generate the P3 response differential and the P3 valuation differential using sLORETA[37] (see STAR Methods). The estimated source of the P3 response differential was deactivation within bilateral motor cortex, which prior studies have associated with motor planning during evidence accumulation[38–40] (Figure 4A). By contrast, the estimated source of the P3 valuation bias was activation of striatum and posterior cingulate cortex (PCC), both of which have been linked to reward processing and representation of subjective value guiding decisions[41,42] (Figure 4B). Thus, P3 response differential and P3 valuation differential index distinct decision biases and appear to originate in brain regions implicated in motor planning and valuation processes, respectively.

P3 differentials characterized distinct types of loss-averse decision makers

In a prior study, we showed that DDM analysis uncovered distinct types of loss-averse decision-makers who were otherwise undetectable based solely on their pattern of choices.[28] Here, we extended that approach by asking whether distinct types of loss-averse decision-makers can be identified solely based on their frontal P3 differentials. Individual participants varied in their combinations of frontal P3 response differential and P3 valuation differential (Figure 5). We highlighted two individuals (Participant 14 and Participant 22) who accepted almost the exact same sets of gambles (Figure 6A), both fewer than half. According to convention, they would be considered similarly loss-averse. By incorporating their response time data into DDM, we found Participant 14 had a larger response bias (Figure 1E, purple dot), whereas Participant 22 had a larger valuation bias (Figure 1E, green dot). Importantly, at the electrophysiological level, we also found a larger P3 response differential in Participant 14 and a larger P3 valuation differential in Participant 22 (Figure 6B). Thus, the P3 response differential and P3

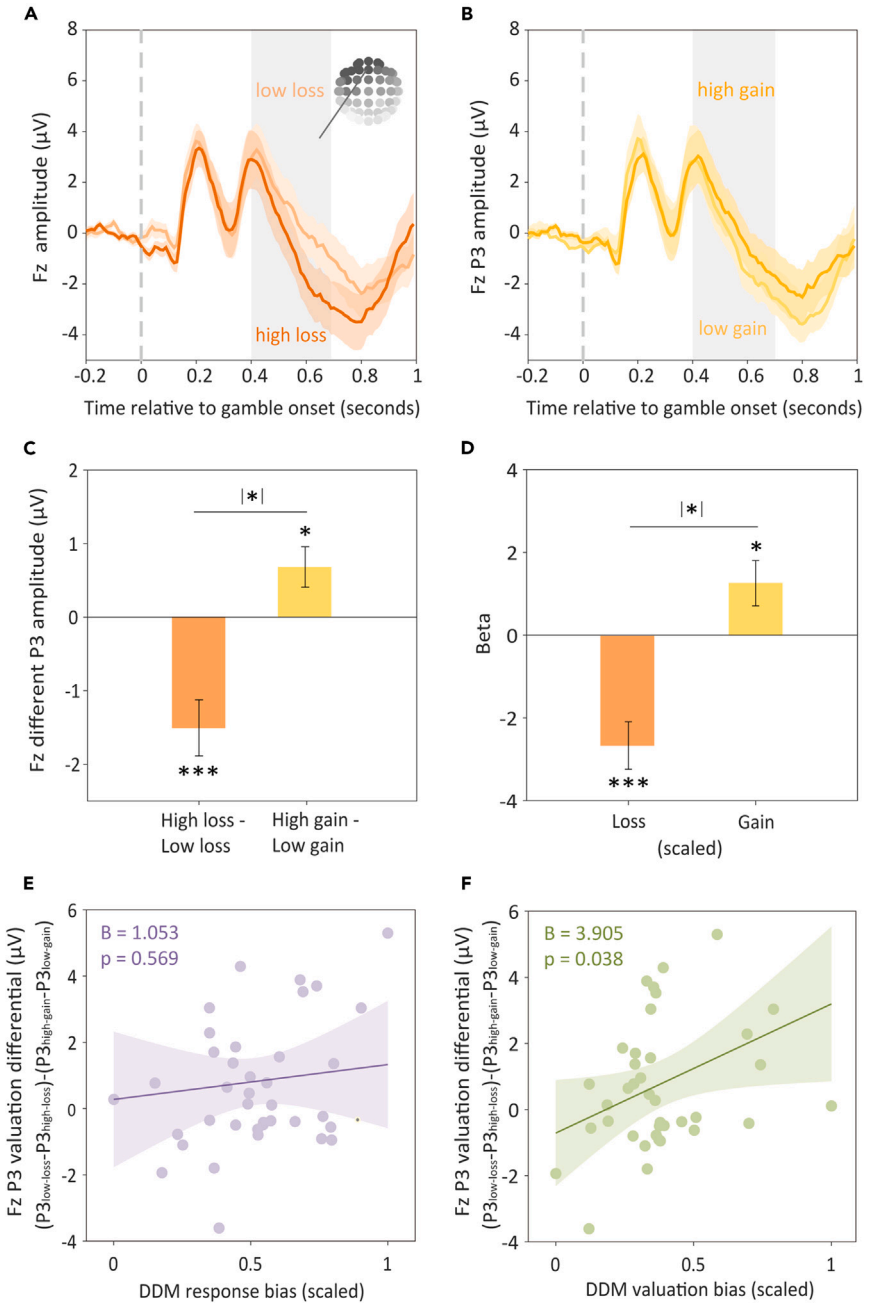

Figure 3. Frontal electrophysiological responses as a function of the magnitudes of potential losses and gains

(A) The mean amplitudes of ERPs locked to the onsets of gambles with low-loss (light orange, ¥10–50) and high-loss (dark orange, ¥60–100), respectively. The topography at the top-right corner indicates P3 valuation differential across electrodes, with the darker gray representing larger values.

(B) The mean amplitudes of ERPs locked to the onsets of gambles with low-gain (light yellow, ¥10–50) and high-gain (dark yellow, ¥60–100), respectively. Shaded areas indicate ±SEM. The gray rectangles (A, B) indicate the window of analysis.

(C) Different P3 amplitude to high-loss vs. low-loss and that to high-gain vs. low gain gambles. Error bars indicate ±SEM. ***$p < 0.001$; *$p < 0.05$. |*| indicates $p < 0.05$ for analyses performed on P3 valuation differential [i.e., (P3low-loss−P3high-loss)−(P3high-gain−P3low-gain)].

(D) Betas estimated by regressing P3 amplitude simultaneously on the magnitudes of gains and losses across trials. Error bars indicate ±SE. |*| indicates $p < 0.05$ for the contrast of the absolute size between the two betas.

(E and F) Relationships between P3 valuation differential and the two DDM biases. The purple (E) and green (F) lines were fitted with a regression simultaneously on DDM response bias and valuation bias that rescaled to values between 0 and 1.

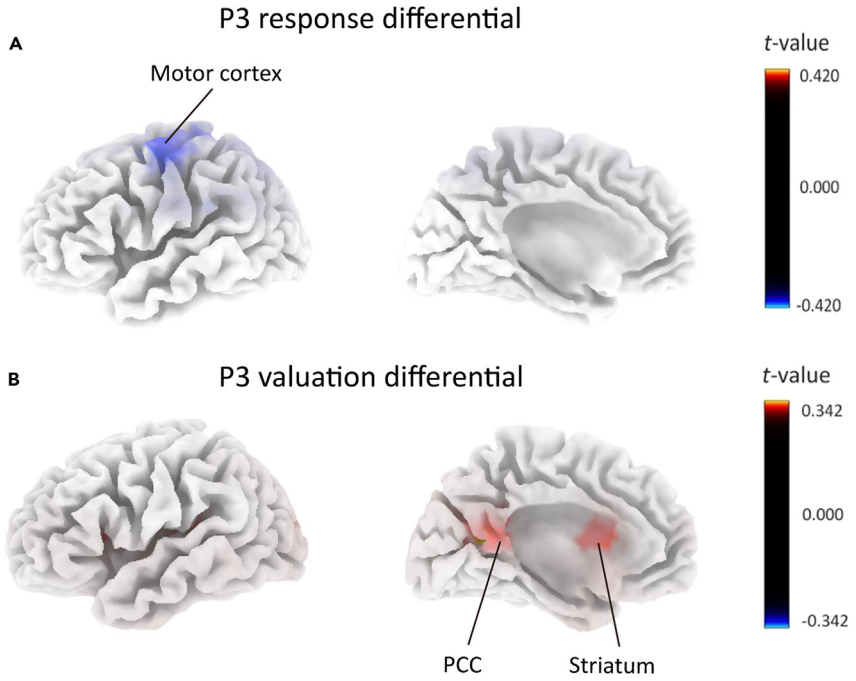

Figure 4. Source localization of P3 differentials

(A) P3 response differential ($P3_{accept}-P3_{reject}$) was associated with deactivation of motor cortex. (B) P3 valuation differential [($P3_{low\text{-}loss}-P3_{high\text{-}loss}$) −($P3_{high\text{-}gain}-P3_{low\text{-}gain}$)] was associated with activation of striatum and posterior cingulate cortex (PCC). Maps are color-coded by SnPM t-values, where blue and red indicate negative and positive values (two-tailed), respectively.

valuation differential provide directly observable biomarkers of individual differences in the processes that generate what are otherwise similar loss-averse decisions.

P3 predicted choice and response time

We next examined whether frontal P3 amplitude predicts choices and response times at the trial level. First, using multi-level logistic regression, we found that larger P3 amplitudes predicted a higher probability of gamble acceptance (Beta = 0.019, SE = 0.004, 95% CI: 0.012 to 0.027, $p < 0.001$). Further, for each individual, we estimated the probability of acceptance for each gamble based on the parameters derived from the logistic regression and then made predictions for each gamble depending on whether the estimated probability of acceptance was larger than 50%, thus accepting the gamble, or not, thus rejecting the gamble. We found prediction accuracy was about 73%, significantly higher than chance (M ± SD = 73.5% ± 9.6%, range: 54.0%–95.5%; t(40) = 15.63, $p < 0.001$). To determine whether P3 amplitude predicts response times in addition to choices, we constructed a DDM (DDM5) that modeled P3 amplitude as an additive component in the drift rate (see STAR Methods). We found this extended DDM outperformed the model that did not incorporate P3 amplitude (DDM4) (ΔDIC = −47.67). Collectively, these results endorse the hypothesis that P3 reflects evidence-accumulation during decisions to accept or reject a gamble and that P3 amplitude predicts both which choice will be made and when it will be made.

We also tested whether, at the individual level, frontal P3 differentials predict probability of gamble acceptance and response time to accept vs. reject gambles—the two behavioral indices of loss aversion without DDM modeling. We found that frontal P3 response differential was negatively correlated with probability of gamble acceptance (r = −0.516, $p = 0.001$) and positively correlated with differential response time to accept vs. reject gambles (r = 0.353, $p = 0.024$). By contrast, frontal P3 valuation differentials were correlated with neither probability of gamble acceptance (r = −0.060, $p = 0.710$) nor differential response time to accept vs. reject gambles (r = 0.186, $p = 0.244$). Thus, frontal P3 response differential was reflected in the two typical behavioral indices of loss aversion without modeling while frontal P3 valuation differential was not.

Loss aversion estimated by prospect theory was correlated with P3 response differential but not P3 valuation differential

Loss aversion in mixed-gamble tasks is conventionally estimated as a single bias by prospect theory (PT), which models choices without taking into account response times.[2] Taking this conventional approach, we found loss aversion, when estimated as log-transformed weighting of loss relative to gain using PT based on choice data alone (see STAR Methods), was correlated with both valuation bias (r = 0.524, $p < 0.001$) and response bias (r = 0.658, $p < 0.001$) estimated by DDM, which replicated our previous finding.[28] We then examined whether PT loss aversion was reflected in P3 differentials. We found that PT loss aversion was correlated with P3 response differential at both the frontal site (r = 0.550,

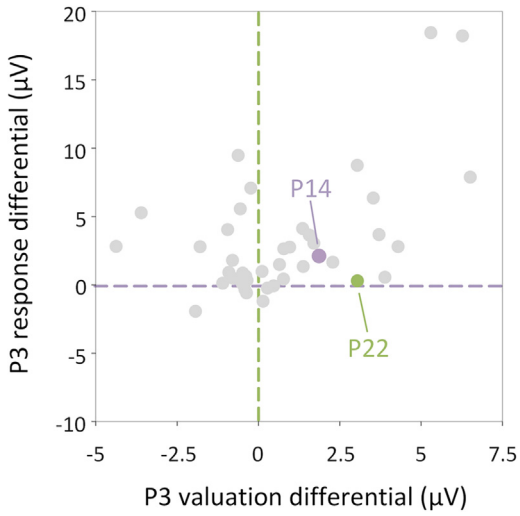

Figure 5. Relationship between P3 valuation differential and P3 response differential
Each point indicates a participant. The purple and green dots represent P14 and P22, respectively.

$p < 0.001$) and the parietal site ($r = 0.539$, $p < 0.001$) but was not correlated with P3 valuation differential at neither frontal nor parietal site (both rs < 0.149, both ps > 0.351). Thus, without modeling response times, we were unable to observe separable behavioral indices of P3 response differential and P3 valuation differential.

Loss aversion was not observed in P2 and N2

Finally, we asked whether loss aversion might also be reflected in ERP components earlier than P3, like P2 and N2, both of which have been previously implicated in processing of risk.[43–47] We calculated the mean P2 amplitude within 200–300 ms and N2 amplitude within 300–400 ms, and for each component, computed response differential (i.e., accept - reject) and valuation differential [i.e., (low-loss−high-loss)−(high-gain−low-gain)] at the frontal site and the parietal site, respectively. We found neither significant response differential nor significant valuation differential of P2 or N2 at either the frontal or the parietal site (all ps > 0.166; see Tables S1 and S2 for details). Thus, in our task, P2 and N2 did not discriminate gamble acceptance and rejection and did not show different sensitivity to the magnitude of losses and the magnitude of gains.

DISCUSSION

Applying an evidence-accumulation framework using DDM and EEG, we decomposed loss aversion from the dynamics of a single scalp electrical signal, P3. Specifically, we observed a response bias to avoid potential losses indexed by larger P3 preceding gamble acceptance than rejection, which was localizable to motor cortex. We further observed a valuation bias to amplify potential losses indexed by larger sensitivity of P3 to potential losses than potential gains, which was localizable to brain regions implicated in reward processing. Our study provides direct neural evidence supporting the hypothesis that loss aversion arises from a combination of response bias and valuation bias and describes neural biomarkers that can identify distinct types of loss-averse decision-makers.

The cognitive mechanisms underlying loss aversion remain hotly debated.[19,21] The conventional account theorizes that loss aversion results from subjective magnification of losses over gains.[2] By contrast, the response-bias account proffers that loss aversion arises from avoidance of any choice that could result in a loss.[17,20] By coupling DDM analysis of both choices and response times with EEG, we uncovered both response bias and valuation bias multiplexed within the dynamics of a single electrical signal, P3. Prior studies demonstrated that P3 reflects the updating of mental states when contexts change[31] and tracks evidence accumulation during perceptual decision-making.[35,48,49] Our study builds upon and extends these findings by linking P3 to evidence accumulation processes during value-based decision-making and invites accommodation with the prevailing mental-updating hypothesis of P3.[31] Specifically, the larger P3 evoked by gamble acceptance than rejection, or P3 response differential, implies that a larger amount of evidence must be accumulated to update the default tendency to reject gambles. The larger sensitivity of P3 to potential losses than potential gains, or P3 valuation differential, suggests potential losses provoke greater mental updating relative to an equivalent amount of potential gains, which was manifest in valuation bias.

The association between P3 and loss aversion was preferentially expressed over frontal cortex. Specifically, response bias was more prominently reflected in frontal than parietal P3 response differentials, and valuation bias was selectively indexed by frontal but not parietal P3 valuation differentials. This is consistent with the observation that evidence accumulation processes are reflected selectively in neural oscillations over frontal areas during value-based decision-making but reflected in neural oscillations over parietal cortex during both perceptual and value-based decision-making.[36] Our findings thus endorse the selectivity of frontal electrical activity for decoding value-based decisions.

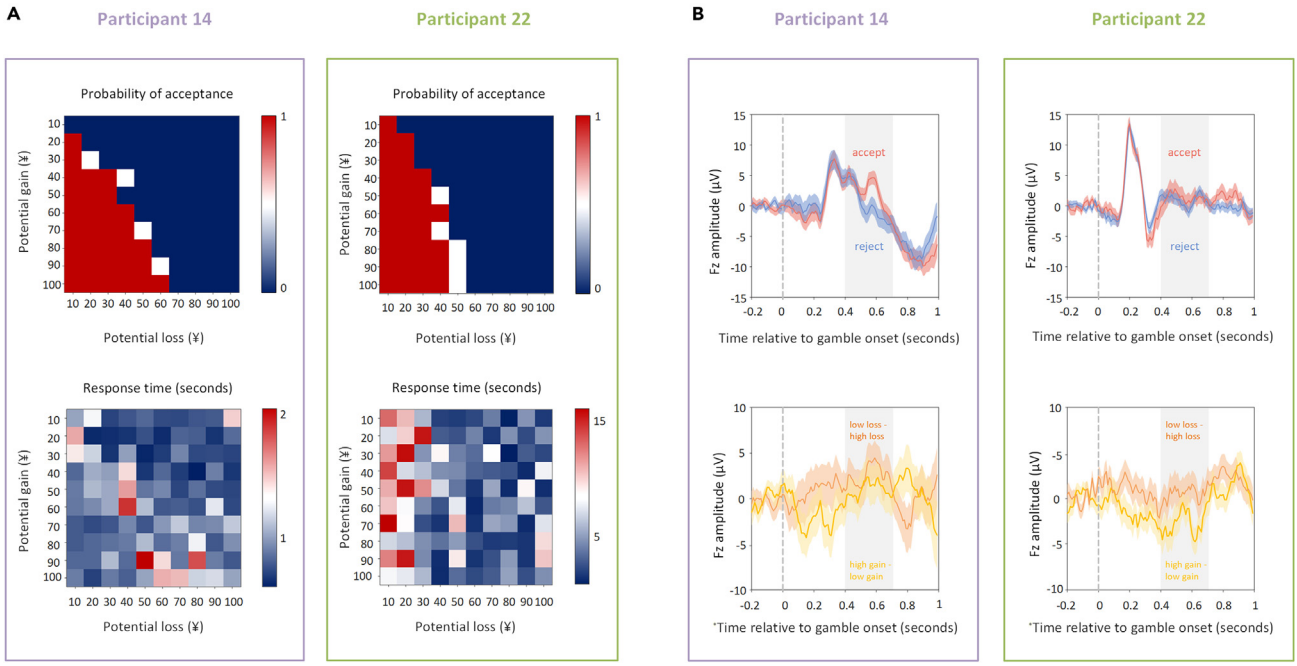

Figure 6. Two example participants

(A) Probability of acceptance and response times of two example participants.

(B) Electrophysiological responses of two example participants. The two pictures above are mean amplitudes of ERPs locked to gamble onset for accepted and rejected gambles, respectively. The two pictures below are different amplitude for low-loss and high-loss gambles and that for high-gain and low-gain gambles, respectively. Shaded areas indicate ±SEM. Gray rectangles indicate the windows of analysis.

The literature on P3 has discriminated an earlier frontocentral subcomponent P3a and a later parietal subcomponent P3b in distinct contexts.[33,50] For example, in oddball tasks, P3b is evoked by the target stimulus, whereas P3a is evoked by a distractor. In addition, in language-comprehension task, a delayed variant of P3b, or P600, is often evoked by syntactic and semantic incongruity.[51] In our gambling task, P3 emerged at a relatively late stage at both the frontal and parietal regions and was larger at the parietal region than over the frontal region (see Figure S2). However, gamble acceptance and rejection (Figure S4) as well as gain and loss magnitude (Figure S6) were better discriminated by frontal P3 than parietal P3. Our findings thus provide a special case for the coexistence and distinction between frontal and parietal P3s and add to the accumulating literature on the subcomponents of P3.

The current study investigated electrophysiological activity alongside the process of decision-making under risk, with a focus on P3, a classic ERP that has been previously found for the selection of riskier options (see ref.[52] for a review). By employing evidence accumulation modeling, we decomposed response bias and valuation bias underpinning P3 in risky decision-making. In addition to the P3 component preceding decisions, two post-decision ERP components have been commonly found for risky decision-making.[52,53] One is error-related negativity (ERN) locked to response, which is often elicited by error commission and has been found to be enhanced for risk taking,[54] and the other is feedback-related negativity (FRN) locked to the onset of outcome, which often displays distinct sensitivity to gains and losses.[54–56] Our decomposition of response bias and valuation bias in risky decision-making provides an integrative framework for future research to examine potentially distinct relationships between the two post-decision electrophysiological components and the two biases. For example, ERN may preferentially reflect response bias, whereas FRN may preferentially reflect valuation bias.

Using source localization, we further showed that P3 response differential and P3 valuation differential most likely arise from distinct brain regions. Specifically, P3 valuation differential was localizable to two regions of the reward system, i.e., the striatum and PCC. This finding is consistent with previous functional neuroimaging data showing larger hemodynamic responses in the striatum to a reduction in losses than to an increase in gains.[4,57] Previous EEG studies on value-based decision-making have found that scalp potentials underpinning subjective valuation often emerge about 300–700 ms after stimulus onset, localizable to another region of the reward system, i.e., ventral medial prefrontal cortex (VMPFC; see ref.[58] for a review). Specifically, an earlier study on food choice showed that the relative weights of taste and health during evidence accumulation identified by DDM were reflected in a positive ERP component over the frontocentral area emerging 500–650 ms after stimulus onset, which was localizable to VMPFC.[59] Our study, together with these earlier studies, suggests that late frontocentral positive ERP components, presumably arising from the reward system, contribute to evidence construction and mediate valuation bias in value-based decision-making.

By contrast, P3 response differential, or the larger P3 amplitude for gamble acceptance relative to rejection, was localizable to primary motor cortex. In other words, gamble rejection evoked stronger activation in motor cortex. This result is consistent with a previous finding

showing that motor cortex, as a typical region involved in evidence accumulation,[60] underpins response bias, or starting point bias, in perceptual decision-making.[61] This finding also aligns with neurological evidence from movement disorders, showing that higher activity in motor cortex reflects a greater behavioral tendency to maintain the status quo rather than to change it (see ref.[62] for a review). Moreover, like response bias in perceptual decision-making,[63–66] response bias in value-based decision-making has been shown to evolve in response to the choices one experiences.[67] More specifically, response bias of rejecting mixed gambles has been found to be adaptive to the context, which is larger when most gambles are of low payoff and smaller when most gambles are of high payoff.[68] Notably, neural activity in motor cortex has also been found to track experienced choices in human decision-making.[61,69] We speculate that in a mixed gamble task of a symmetric design (Figures 1B and 1C), a typical loss-averse decision-maker may rapidly discover most gambles are not appealing, which potentiates the action that maintains the status quo, manifesting as increased activation of motor cortex.

Our finding that P3 differentially reflects response bias and valuation bias complements our prior findings showing that pupil dilation and gaze allocation index loss-averse decisions. P3 and pupil dilation evoked in decision tasks[70,71] are thought to reflect phasic norepinephrine activity arising from the locus coeruleus.[32] Both P3 amplitude and pupil dynamics track evidence integration[72,73] and reflect mental updating during decision-making.[74–76] P3 amplitude is also modulated by attention,[33] which is indexed by gaze allocation associated with dopaminergic activity.[29] Together, while our former study[28] suggested that response bias and valuation bias underlying loss aversion are indexed by pupil dilation and gaze allocation, respectively, the current study shows that both biases can be reflected in a single neural response, previously found to be related to both types of eye activities.

Notably, the decomposition of response bias and valuation bias from P3 dynamics enabled us to distinguish distinct types of loss-averse decision-makers who would otherwise be indistinguishable from examining decisions alone. An individual with a large valuation bias and a small response bias would be indistinguishable from another individual with a large response bias and a small valuation bias solely based on their choices. In an extreme case, the counteraction of the two biases could, in theory, result in no behavioral evidence of loss aversion. The P3 response differential and valuation differential can resolve these situations. Thus, our two-dimensional model provides a neurophysiologically grounded framework for discriminating the nuanced differences between distinct types of loss-averse decision-makers.

P3 is one of the most commonly used ERP signals for clinical assessment of psychiatric symptoms[77] such as depression,[78,79] schizophrenia,[80–82] and obsessive-compulsive disorder.[81,83] In parallel, loss aversion is one of the most common decision biases linked to these psychiatric conditions.[10,11,14–16] Here, by integrating decision-making, EEG, and computational modeling, we offer a theoretical framework and a scalable measure that may prove useful for clinical research and treatment. Our study thus demonstrates how decision neuroscience can contribute to the emerging field of computational psychiatry.

Limitations of the study

By leveraging high temporal resolution of scalp EEG, we unfolded the time course of loss-averse decisions with a focus on P3 and dissociated valuation bias and response bias that were localizable to the reward system and the motor system, respectively. Yet, there are two limitations of our scalp-EEG-based approach. First, source localization of scalp EEG could only be suggestive but not demonstrative about the activity of the brain structures underlying the skull. Building on our behavioral paradigm and computational model, follow-up studies may utilize intracranial EEG or fMRI to scrutinize the neuroanatomical correlates of the two biases underpinning loss-averse decisions. Second, the observed association between scalp neuroelectrical signals and loss aversion is correlational but not necessarily causal. Future studies may employ techniques manipulative of neurophysiological activity to test potential causal relationship.

STAR★METHODS

Detailed methods are provided in the online version of this paper and include the following:

- KEY RESOURCES TABLE
- RESOURCE AVAILABILITY
  - Lead contact
  - Materials availability
  - Data and code availability
- EXPERIMENTAL MODEL AND STUDY PARTICIPANT DETAILS
- METHOD DETAILS
  - Task
  - EEG data recording
- QUANTIFICATION AND STATISTICAL ANALYSIS
  - EEG data analyses
  - DDM
  - Prospect theory model
  - T-tests and regression analyses

SUPPLEMENTAL INFORMATION

Supplemental information can be found online at https://doi.org/10.1016/j.isci.2024.110153.

ACKNOWLEDGMENTS

We thank Elizabeth M. Brannon for critical comments on the manuscript. This work is supported by NSFC 32200883 to F.S., STI 2030-Major Projects 2021ZD0200409 to F.S. and X.W., NSFC 72072161 to X.W., R01MH108627 to M.L.P., Fundamental Research Funds for Central Universities of China and MOE Frontiers Science Center for Brain Science & Brain-Machine Integration at Zhejiang University.

AUTHOR CONTRIBUTIONS

F.S. conceived the study; R.W., X.W., and F.S. designed the experiment; R.W. conducted the experiment; R.W., X.W., and F.S. analyzed the data; R.W., X.W., M.L.P., and F.S. wrote the manuscript; F.S. supervised the project.

DECLARATION OF INTERESTS

M.L.P. is a scientific advisory board member, consultant, and/or co-founder of Blue Horizons International, NeuroFlow, Amplio, Cogwear Technologies, Burgeon Labs, and Glassview and receives research funding from AIIR Consulting, the SEB Group, Mars Inc, Slalom Inc, and Benjamin Franklin Technology Partners. All other authors declare no competing interests.

Received: September 12, 2023
Revised: April 19, 2024
Accepted: May 28, 2024
Published: June 6, 2024

REFERENCES

1. Kahneman, D., and Tversky, A. (1979). Prospect theory: An analysis of decision under risk. Econometrica *47*, 263–292.
2. Tversky, A., and Kahneman, D. (1992). Advances in prospect theory: Cumulative representation of uncertainty. J. Risk Uncertain. *5*, 297–323. https://doi.org/10.1007/BF00122574.
3. De Martino, B., Camerer, C.F., and Adolphs, R. (2010). Amygdala damage eliminates monetary loss aversion. Proc. Natl. Acad. Sci. USA *107*, 3788–3792. https://doi.org/10.1073/pnas.0910230107.
4. Tom, S.M., Fox, C.R., Trepel, C., and Poldrack, R.A. (2007). The neural basis of loss aversion in decision-making under risk. Science *315*, 515–518. https://doi.org/10.1126/science.1134239.
5. Benartzi, S., and Thaler, R.H. (1995). Myopic loss aversion and the equity premium puzzle. Q. J. Econ. *110*, 73–92. https://doi.org/10.2307/2118511.
6. Hardie, B.G.S., Johnson, E.J., and Fader, P.S. (1993). Modeling loss aversion and reference dependence effects on brand choice. Market. Sci. *12*, 378–394. https://doi.org/10.1287/mksc.12.4.378.
7. Odean, T. (1998). Are investors reluctant to realize their losses? J. Finance *53*, 1775–1798. https://doi.org/10.1111/0022-1082.00072.
8. Brosnan, S.F., Jones, O.D., Lambeth, S.P., Mareno, M.C., Richardson, A.S., and Schapiro, S.J. (2007). Endowment effects in chimpanzees. Curr. Biol. *17*, 1704–1707.
9. Chen, M.K., Lakshminarayanan, V., and Santos, L.R. (2006). How basic are behavioral biases? Evidence from capuchin monkey trading behavior. J. Polit. Econ. *114*, 517–537. https://doi.org/10.1086/503550.
10. Chandrasekhar Pammi, V.S., Pillai Geethabhavan Rajesh, P., Kesavadas, C., Rappai Mary, P., Seema, S., Radhakrishnan, A., and Sitaram, R. (2015). Neural loss aversion differences between depression patients and healthy individuals: A functional MRI investigation. NeuroRadiol. J. *28*, 97–105. https://doi.org/10.1177/1971400915576670.
11. Huh, H.J., Baek, K., Kwon, J.-H., Jeong, J., and Chae, J.-H. (2016). Impact of childhood trauma and cognitive emotion regulation strategies on risk-aversive and loss-aversive patterns of decision-making in patients with depression. Cogn. Neuropsychiatry *21*, 447–461. https://doi.org/10.1080/13546805.2016.1230053.
12. Charpentier, C.J., De Martino, B., Sim, A.L., Sharot, T., and Roiser, J.P. (2016). Emotion-induced loss aversion and striatal-amygdala coupling in low-anxious individuals. Soc. Cogn. Affect. Neurosci. *11*, 569–579. https://doi.org/10.1093/scan/nsv139.
13. Xu, P., Van Dam, N.T., van Tol, M.-J., Shen, X., Cui, Z., Gu, R., Qin, S., Aleman, A., Fan, J., and Luo, Y.J. (2020). Amygdala-prefrontal connectivity modulates loss aversion bias in anxious individuals. Neuroimage *218*, 116957. https://doi.org/10.1016/j.neuroimage.2020.116957.
14. Currie, J., Waiter, G.D., Johnston, B., Feltovich, N., and Douglas Steele, J. (2022). Blunted neuroeconomic loss aversion in schizophrenia. Brain Res. *1789*, 147957. https://doi.org/10.1016/j.brainres.2022.147957.
15. Trémeau, F., Brady, M., Saccente, E., Moreno, A., Epstein, H., Citrome, L., Malaspina, D., and Javitt, D. (2008). Loss aversion in schizophrenia. Schizophr. Res. *103*, 121–128. https://doi.org/10.1016/j.schres.2008.03.027.
16. Sip, K.E., Gonzalez, R., Taylor, S.F., and Stern, E.R. (2017). Increased loss aversion in unmedicated patients with obsessive-compulsive disorder. Front. Psychiatry *8*, 309. https://doi.org/10.3389/fpsyt.2017.00309.
17. Ert, E., and Erev, I. (2008). The rejection of attractive gambles, loss aversion, and the lemon avoidance heuristic. J. Econ. Psychol. *29*, 715–723. https://doi.org/10.1016/j.joep.2007.06.003.
18. Gal, D. (2006). A psychological law of inertia and the illusion of loss aversion. Judgm. Decis. Making *1*, 23–32. https://doi.org/10.1017/S1930297500000322.
19. Gal, D., and Rucker, D.D. (2018). The loss of loss aversion: Will it loom larger than its gain? J. Consum. Psychol. *28*, 497–516. https://doi.org/10.1002/jcpy.1047.
20. Ritov, I., and Baron, J. (1992). Status-quo and omission biases. J. Risk Uncertain. *5*, 49–61. https://doi.org/10.1007/BF00208786.
21. Yechiam, E. (2019). Acceptable losses: The debatable origins of loss aversion. Psychol. Res. *83*, 1327–1339. https://doi.org/10.1007/s00426-018-1013-8.
22. Chrousos, G.P. (2009). Stress and disorders of the stress system. Nat. Rev. Endocrinol. *5*, 374–381. https://doi.org/10.1038/nrendo.2009.106.
23. Takahashi, H., Fujie, S., Camerer, C., Arakawa, R., Takano, H., Kodaka, F., Matsui, H., Ideno, T., Okubo, S., Takemura, K., et al. (2013). Norepinephrine in the brain is associated with aversion to financial loss. Mol. Psychiatry *18*, 3–4. https://doi.org/10.1038/mp.2012.7.
24. Sokol-Hessner, P., Lackovic, S.F., Tobe, R.H., Camerer, C.F., Leventhal, B.L., and Phelps, E.A. (2015). Determinants of propranolol's selective effect on loss aversion. Psychol. Sci. *26*, 1123–1130. https://doi.org/10.1177/0956797615582026.
25. Sokol-Hessner, P., Hsu, M., Curley, N.G., Delgado, M.R., Camerer, C.F., and Phelps, E.A. (2009). Thinking like a trader selectively reduces individuals' loss aversion. Proc. Natl. Acad. Sci. USA *106*, 5035–5040. https://doi.org/10.1073/pnas.0806761106.
26. Gold, J.I., and Shadlen, M.N. (2007). The neural basis of decision making. Annu. Rev. Neurosci. *30*, 535–574.
27. Ratcliff, R., Smith, P.L., Brown, S.D., and McKoon, G. (2016). Diffusion decision model: Current issues and history. Trends Cogn. Sci. *20*, 260–281.
28. Sheng, F., Ramakrishnan, A., Seok, D., Zhao, W.J., Thelaus, S., Cen, P., and Platt, M.L. (2020). Decomposing loss aversion from gaze allocation and pupil dilation. Proc. Natl. Acad. Sci. USA *117*, 11356–11363.
29. Westbrook, A., van den Bosch, R., Määttä, J.I., Hofmans, L., Papadopetraki, D., Cools, R., and Frank, M.J. (2020). Dopamine promotes cognitive effort by biasing the benefits versus

costs of cognitive work. Science *367*, 1362–1366. https://doi.org/10.1126/science.aaz5891.
30. Joshi, S., and Gold, J.I. (2020). Pupil size as a window on neural substrates of cognition. Trends Cogn. Sci. *24*, 466–480. https://doi.org/10.1016/j.tics.2020.03.005.
31. Donchin, E., and Coles, M.G.H. (1988). Is the P300 component a manifestation of context updating? Behav. Brain Sci. *11*, 357–374. https://doi.org/10.1017/S0140525X00058027.
32. Nieuwenhuis, S., Aston-Jones, G., and Cohen, J.D. (2005). Decision making, the P3, and the locus coeruleus-norepinephrine system. Psychol. Bull. *131*, 510–532. https://doi.org/10.1037/0033-2909.131.4.510.
33. Polich, J. (2007). Updating P300 : An integrative theory of P3a and P3b. Clin. Neurophysiol. *118*, 2128–2148. https://doi.org/10.1016/j.clinph.2007.04.019.
34. Donchin, E. (1981). Surprise!.Surprise? Psychophysiology *18*, 493–513.
35. Twomey, D.M., Murphy, P.R., Kelly, S.P., and O'Connell, R.G. (2015). The classic P300 encodes a build-to-threshold decision variable. Eur. J. Neurosci. *42*, 1636–1643. https://doi.org/10.1111/ejn.12936.
36. Polanía, R., Krajbich, I., Grueschow, M., and Ruff, C.C. (2014). Neural oscillations and synchronization differentially support evidence accumulation in perceptual and value-based decision making. Neuron *82*, 709–720. https://doi.org/10.1016/j.neuron.2014.03.014.
37. Pascual-Marqui, R.D. (2002). Standardized low-resolution brain electromagnetic tomography (sLORETA): Technical details. Methods Find. Exp. Clin. Pharmacol. *24*, 5–12.
38. Donner, T.H., Siegel, M., Fries, P., and Engel, A.K. (2009). Buildup of choice-predictive activity in human motor cortex during perceptual decision making. Curr. Biol. *19*, 1581–1585. https://doi.org/10.1016/j.cub.2009.07.066.
39. Thura, D., and Cisek, P. (2016). Modulation of premotor and primary motor cortical activity during volitional adjustments of speed-accuracy trade-offs. J. Neurosci. *36*, 938–956. https://doi.org/10.1523/JNEUROSCI.2230-15.2016.
40. Wyart, V., de Gardelle, V., Scholl, J., and Summerfield, C. (2012). Rhythmic fluctuations in evidence accumulation during decision making in the human brain. Neuron *76*, 847–858. https://doi.org/10.1016/j.neuron.2012.09.015.
41. Levy, D.J., and Glimcher, P.W. (2012). The root of all value: A neural common currency for choice. Curr. Opin. Neurobiol. *22*, 1027–1038. https://doi.org/10.1016/j.conb.2012.06.001.
42. Rangel, A., Camerer, C., and Montague, P.R. (2008). A framework for studying the neurobiology of value-based decision making. Nat. Rev. Neurosci. *9*, 545–556. https://doi.org/10.1038/nrn2357.
43. Qin, J., and Han, S. (2009). Neurocognitive mechanisms underlying identification of environmental risks. Neuropsychologia *47*, 397–405. https://doi.org/10.1016/j.neuropsychologia.2008.09.010.
44. Bian, J., Fu, H., and Jin, J. (2020). Are we sensitive to different types of safety signs? Evidence from ERPs. Psychol. Res. Behav. Manag. *13*, 495–505. https://doi.org/10.2147/PRBM.S248947.
45. Zhang, S., Yu, X., Shi, X., and Zhang, Y. (2023). The influencing mechanism of incidental emotions on risk perception: Evidence from event-related potential. Brain Sci. *13*, 486. https://doi.org/10.3390/brainsci13030486.
46. Ma, Q., Pei, G., and Wang, K. (2015). Influence of negative emotion on the framing effect: Evidence from event-related potentials. Neuroreport *26*, 325–332. https://doi.org/10.1097/WNR.0000000000000346.
47. Yang, J., Li, H., Zhang, Y., Qiu, J., and Zhang, Q. (2007). The neural basis of risky decision-making in a blackjack task. Neuroreport *18*, 1507–1510. https://doi.org/10.1097/WNR.0b013e3282ef7565.
48. Kelly, S.P., Corbett, E.A., and O'Connell, R.G. (2021). Neurocomputational mechanisms of prior-informed perceptual decision-making in humans. Nat. Hum. Behav. *5*, 467–481. https://doi.org/10.1038/s41562-020-00967-9.
49. O'Connell, R.G., Dockree, P.M., and Kelly, S.P. (2012). A supramodal accumulation-to-bound signal that determines perceptual decisions in humans. Nat. Neurosci. *15*, 1729–1735. https://doi.org/10.1038/nn.3248.
50. Squires, N.K., Squires, K.C., and Hillyard, S.A. (1975). Two varieties of long-latency positive waves evoked by unpredictable auditory stimuli in man. Electroencephalogr. Clin. Neurophysiol. *38*, 387–401. https://doi.org/10.1016/0013-4694(75)90263-1.
51. Leckey, M., and Federmeier, K.D. (2020). The P3b and P600(s): Positive contributions to language comprehension. Psychophysiology *57*, e13351. https://doi.org/10.1111/psyp.13351.
52. Chandrakumar, D., Feuerriegel, D., Bode, S., Grech, M., and Keage, H.A.D. (2018). Event-related potentials in relation to risk-taking: A systematic review. Front. Behav. Neurosci. *12*, 111.
53. Walsh, M.M., and Anderson, J.R. (2012). Learning from experience: Event-related potential correlates of reward processing, neural adaptation, and behavioral choice. Neurosci. Biobehav. Rev. *36*, 1870–1884.
54. Yu, R., and Zhou, X. (2009). To bet or not to bet? The error negativity or error-related negativity associated with risk-taking choices. J. Cogn. Neurosci. *21*, 684–696. https://doi.org/10.1162/jocn.2009.21034.
55. Yaple, Z., Shestakova, A., and Klucharev, V. (2018). Feedback-related negativity reflects omission of monetary gains: Evidence from ERP gambling study. Neurosci. Lett. *686*, 145–149. https://doi.org/10.1016/j.neulet.2018.09.007.
56. Gehring, W.J., and Willoughby, A.R. (2002). The medial frontal cortex and the rapid processing of monetary gains and losses. Science *295*, 2279–2282. https://doi.org/10.1126/science.1066893.
57. Canessa, N., Crespi, C., Motterlini, M., Baud-Bovy, G., Chierchia, G., Pantaleo, G., Tettamanti, M., and Cappa, S.F. (2013). The functional and structural neural basis of individual differences in loss aversion. J. Neurosci. *33*, 14307–14317. https://doi.org/10.1523/JNEUROSCI.0497-13.2013.
58. Harris, A., and Hutcherson, C.A. (2022). Temporal dynamics of decision making: A synthesis of computational and neurophysiological approaches. Wiley Interdiscip. Rev. Cogn. Sci. *13*, e1586. https://doi.org/10.1002/wcs.1586.
59. Harris, A., Clithero, J.A., and Hutcherson, C.A. (2018). Accounting for taste: A multi-attribute neurocomputational model explains the neural dynamics of choices for self and others. J. Neurosci. *38*, 7952–7968. https://doi.org/10.1523/JNEUROSCI.3327-17.2018.
60. Hanks, T.D., and Summerfield, C. (2017). Perceptual decision making in rodents, monkeys, and humans. Neuron *93*, 15–31. https://doi.org/10.1016/j.neuron.2016.12.003.
61. de Lange, F.P., Rahnev, D.A., Donner, T.H., and Lau, H. (2013). Prestimulus oscillatory activity over motor cortex reflects perceptual expectations. J. Neurosci. *33*, 1400–1410. https://doi.org/10.1523/JNEUROSCI.1094-12.2013.
62. Engel, A.K., and Fries, P. (2010). Beta-band oscillations—signalling the status quo? Curr. Opin. Neurobiol. *20*, 156–165. https://doi.org/10.1016/j.conb.2010.02.015.
63. Cho, R.Y., Nystrom, L.E., Brown, E.T., Jones, A.D., Braver, T.S., Holmes, P.J., and Cohen, J.D. (2002). Mechanisms underlying dependencies of performance on stimulus history in a two-alternative forced-choice task. Cogn. Affect. Behav. Neurosci. *2*, 283–299. https://doi.org/10.3758/cabn.2.4.283.
64. Gold, J.I., Law, C.-T., Connolly, P., and Bennur, S. (2008). The relative influences of priors and sensory evidence on an oculomotor decision variable during perceptual learning. J. Neurophysiol. *100*, 2653–2668. https://doi.org/10.1152/jn.90629.2008.
65. Yu, A.J., and Cohen, J.D. (2008). Sequential effects: Superstition or rational behavior? Adv. Neural Inf. Process. Syst. *21*, 1873–1880.
66. Gao, J., Wong-Lin, K., Holmes, P., Simen, P., and Cohen, J.D. (2009). Sequential effects in two-choice reaction time tasks: Decomposition and synthesis of mechanisms. Neural Comput. *21*, 2407–2436. https://doi.org/10.1162/neco.2009.09-08-866.
67. Desai, N., and Krajbich, I. (2022). Decomposing preferences into predispositions and evaluations. J. Exp. Psychol. Gen. *151*, 1883–1903. https://doi.org/10.1037/xge0001162.
68. Zhao, W.J., Walasek, L., and Bhatia, S. (2020). Psychological mechanisms of loss aversion: A drift-diffusion decomposition. Cogn. Psychol. *123*, 101331. https://doi.org/10.1016/j.cogpsych.2020.101331.
69. Akaishi, R., Umeda, K., Nagase, A., and Sakai, K. (2014). Autonomous mechanism of internal choice estimate underlies decision inertia. Neuron *81*, 195–206. https://doi.org/10.1016/j.neuron.2013.10.018.
70. Steinhauer, S.R., and Hakerem, G. (1992). The pupillary response in cognitive psychophysiology and schizophrenia. Ann. N. Y. Acad. Sci. *658*, 182–204.
71. Kamp, S.M., and Donchin, E. (2015). ERP and pupil responses to deviance in an oddball paradigm. Psychophysiology *52*, 460–471. https://doi.org/10.1111/psyp.12378.
72. Keung, W., Hagen, T.A., and Wilson, R.C. (2019). Regulation of evidence accumulation by pupil-linked arousal processes. Nat. Hum. Behav. *3*, 636–645. https://doi.org/10.1038/s41562-019-0551-4.
73. de Gee, J.W., Colizoli, O., Kloosterman, N.A., Knapen, T., Nieuwenhuis, S., and Donner, T.H. (2017). Dynamic modulation of decision biases by brainstem arousal systems. Elife *6*, e23232. https://doi.org/10.7554/eLife.23232.
74. Chen, W.J., and Krajbich, I. (2017). Computational modeling of epiphany learning. Proc. Natl. Acad. Sci. USA *114*, 4637–4642. https://doi.org/10.1073/pnas.1618161114.

75. de Gee, J.W., Correa, C.M.C., Weaver, M., Donner, T.H., and van Gaal, S. (2021). Pupil dilation and the slow wave ERP reflect surprise about choice outcome resulting from intrinsic variability in decision confidence. Cereb. Cortex *31*, 3565–3578. https://doi.org/10.1093/cercor/bhab032.
76. de Gee, J.W., Knapen, T., and Donner, T.H. (2014). Decision-related pupil dilation reflects upcoming choice and individual bias. Proc. Natl. Acad. Sci. USA *111*, E618–E625. https://doi.org/10.1073/pnas.1317557111.
77. Polich, J., and Herbst, K.L. (2000). P300 as a clinical assay: Rationale, evaluation, and findings. Int. J. Psychophysiol. *38*, 3–19. https://doi.org/10.1016/S0167-8760(00)00127-6.
78. Bruder, G.E., Tenke, C.E., Stewart, J.W., Towey, J.P., Leite, P., Voglmaier, M., and Quitkin, F.M. (1995). Brain event-related potentials to complex tones in depressed patients: Relations to perceptual asymmetry and clinical features. Psychophysiology *32*, 373–381. https://doi.org/10.1111/j.1469-8986.1995.tb01220.x.
79. Santopetro, N.J., Brush, C.J., Bruchnak, A., Klawohn, J., and Hajcak, G. (2021). A reduced P300 prospectively predicts increased depressive severity in adults with clinical depression. Psychophysiology *58*, e13767. https://doi.org/10.1111/psyp.13767.
80. Jeon, Y.-W., and Polich, J. (2003). Meta-analysis of P300 and schizophrenia: Patients, paradigms, and practical implications. Psychophysiology *40*, 684–701. https://doi.org/10.1111/1469-8986.00070.
81. Kim, M.-S., Kang, S.-S., Youn, T., Kang, D.-H., Kim, J.-J., and Kwon, J.S. (2003). Neuropsychological correlates of P300 abnormalities in patients with schizophrenia and obsessive–compulsive disorder. Psychiatry Res. *123*, 109–123. https://doi.org/10.1016/S0925-4927(03)00045-3.
82. Towey, J.P., Tenke, C.E., Bruder, G.E., Leite, P., Friedman, D., Liebowitz, M., and Hollander, E. (1994). Brain event-related potential correlates of overfocused attention in obsessive-compulsive disorder. Psychophysiology *31*, 535–543. https://doi.org/10.1111/j.1469-8986.1994.tb02346.x.
83. Ford, J.M., White, P.M., Csernansky, J.G., Faustman, W.O., Roth, W.T., and Pfefferbaum, A. (1994). ERPs in schizophrenia: Effects of antipsychotic medication. Biol. Psychiatry *36*, 153–170. https://doi.org/10.1016/0006-3223(94)91221-1.
84. Peirce, J., Gray, J.R., Simpson, S., MacAskill, M., Höchenberger, R., Sogo, H., Kastman, E., and Lindeløv, J.K. (2019). PsychoPy2: Experiments in behavior made easy. Behav. Res. Methods *51*, 195–203. https://doi.org/10.3758/s13428-018-01193-y.
85. Delorme, A., and Makeig, S. (2004). EEGLAB: An open source toolbox for analysis of single-trial EEG dynamics including independent component analysis. J. Neurosci. Methods *134*, 9–21. https://doi.org/10.1016/j.jneumeth.2003.10.009.
86. Fuchs, M., Kastner, J., Wagner, M., Hawes, S., and Ebersole, J.S. (2002). A standardized boundary element method volume conductor model. Clin. Neurophysiol. *113*, 702–712. https://doi.org/10.1016/S1388-2457(02)00030-5.
87. Mazziotta, J., Toga, A., Evans, A., Fox, P., Lancaster, J., Zilles, K., Woods, R., Paus, T., Simpson, G., Pike, B., et al. (2001). A probabilistic atlas and reference system for the human brain: International Consortium for Brain Mapping (ICBM). Philos. Trans. R. Soc. Lond. B Biol. Sci. *356*, 1293–1322. https://doi.org/10.1098/rstb.2001.0915.
88. Thatcher, R.W., North, D., and Biver, C. (2005). Parametric vs. non-parametric statistics of low resolution electromagnetic tomography (LORETA). Clin. EEG Neurosci. *36*, 1–8. https://doi.org/10.1177/155005940503600103.
89. Wiecki, T.V., Sofer, I., and Frank, M.J. (2013). HDDM: Hierarchical bayesian estimation of the drift-diffusion model in Python. Front. Neuroinform. *7*, 14. https://doi.org/10.3389/fninf.2013.00014.

STAR★METHODS

KEY RESOURCES TABLE

REAGENT or RESOURCE	SOURCE	IDENTIFIER
Deposited data		
Behavioral and EEG data	This paper	https://osf.io/ruwe8
Software and algorithms		
MATLAB R2019a	Mathworks, MA, USA	https://matlab.mathworks.com
Psychopy2	Peirce et al.[84]	https://www.psychopy.org
EEGLAB	Delorme and Makeig[85]	https://sccn.ucsd.edu/eeglab/index.php
Original code	This paper	https://osf.io/ruwe8

RESOURCE AVAILABILITY

Lead contact

Further information and requests for resources should be directed to and will be fulfilled by the lead contact, Dr. Feng Sheng (fsheng@zju.edu.cn).

Materials availability

This study did not generate new unique reagents.

Data and code availability

- De-identified behavioral and EEG data have been deposited at Open Science Framework (https://osf.io/ruwe8/) and are publicly available as of the date of publication.
- All original code has been deposited at Open Science Framework (https://osf.io/ruwe8/) and is publicly available as of the date of publication.
- Any additional information required to reanalyze the data reported in this paper is available from the lead contact upon request.

EXPERIMENTAL MODEL AND STUDY PARTICIPANT DETAILS

The protocol of this research was approved by the Ethics Committee of School of Management at Zhejiang University. The experiment was performed in accordance with relevant guidelines and regulations. Informed consents were obtained from all participants. Forty-one adults (all Han Chinese; 26 males, 15 females; 20-26 y, M $\pm$ SD = 23.07 $\pm$ 1.56 y) were recruited. All participants were healthy and right-handed, with normal or corrected-to-normal vision.

METHOD DETAILS

Task

Each participant received ¥100 as an endowment. They were then seated in a dimly lit, electrically shielded room and completed the gambling task on a computer. In each trial, the computer screen displayed a gamble of equal odds to win an amount of money and lose another amount of money (Figure 1A). Participants decided whether to accept or reject the gamble by pressing one of two buttons by the right hand. The amounts of gains and losses both ranged from ¥10 to ¥100, with ¥10 increments, resulting in 100 unique gambles. Each participant completed two blocks of 100 gambles and made decisions twice for each gamble. The order of gambles was randomized for each block and each participant. The positions of gain and loss (i.e., left vs. right, Figure 1A) were fixed within a block, but were switched between the two blocks for each participant. Specifically, for 22 out of 41 participants, gain was displayed on the left in the first block and on the right in the second block. For the other 19 participants, gain was diaplayed on the right in the first block and on the left in the second block. A fixation cross was presented between trials with a varying duration of 2 $\sim$ 4 s. A 5-min break was inserted between the two blocks. The procedures were run by PsychoPy2 (https://www.psychopy.org/).[84]

A gamble was not resolved immediately after a decision was made. Instead, for each participant, after all decisions were made, one of the decisions was randomly selected for payout. When the selelcted decision was rejection, the participant left with the endowed ¥100. When the decision was acceptance, a coin was flipped to determine whether the participant won or lost money. When the coin landed with heads, the participant was paid with the corresponding amount of money in addition to the ¥100 endowment. When the coin landed with tails, the corresponding loss was subtracted from the ¥100 endowment. Participants learned the rule of payment before they started the gambling task.

EEG data recording

The EEG was continuously recorded from 62 Ag/AgCl scalp electrodes mounted on an elastic cap in accordance with the standard 10–20 system (NeuroScan 4.3.1; band pass: 0.05–100 Hz; sampling rate: 1000 Hz). Horizontal electrooculograms (EOGs) were recorded from the electrodes located near the outer canthus each eye, and the vertical EOGs were recorded by the ones above and below the left eye in parallel with the pupil. The electrode impedance was kept below 5 kΩ.

QUANTIFICATION AND STATISTICAL ANALYSIS

EEG data analyses

Recorded EEG was preprocessed offline using EEGLAB.[85] EEG signals recorded from all electrodes were re-referenced to the left and right mastoids, and signals were band-pass filtered (1-40 Hz). Artifacts were removed using MARA plug-in of EEGLAB (freely available at https://irenne.github.io/artifacts) but no trial was removed. ERP at each electrode was identified for each trial from 200 ms before gamble onset to 1000 ms after, with the 200 ms before gamble onset as the baseline. The means and standard deviations of the numbers of epochs identified for gamble acceptance and rejection were 53.6±19.4 and 146.4±19.4, respectively. The numbers of epochs identified for high-gain, low-gain, high-loss and low-loss gambles were 100, 100, 100 and 100, respectively.

For statistical analysis of ERPs, we selected Fz and Pz as electrodes of interests, to denote the frontal and parietal areas, respectively. ERPs at the central area (Cz) showed amplitudes between those at frontal area and those at parietal area, and were thus not additionally reported. 400-700 ms was selected as the window of interests for P3 based on visual inspection. The reported results were robust to the adjustment of the time window.

Source localization was implemented with sLORETA.[37] sLORETA calculates the standardized source current dipole moments at each of the 6239 gray matter voxels with a spatial resolution of 5 mm. Source current dipole moments in each voxel are then calculated in a realistic head model with the probabilistic MNI152 template.[86,87] Specifically, we assessed the 3D current source of neural activity in the window of interests (400-700 ms) that differentiated (1) ERPs to acceptance and rejection, and (2) ERPs to (low loss – high loss) and (high gain – low gain) across participants. All 62 electrodes were used as entries to the data matrix. Comparisons between different stimulus conditions were conducted by the statistical nonparametric mapping (SnPM) test using the log of the ratio of averages (log of F-ratio).[88] The maps were color-coded by the SnPM t-values (Figure 4).

DDM

The main model (DDM4) was adopted from our earlier work,[28] in which the decision to accept or reject a mixed gamble was assumed as the outcome of a noisy evidence accumulation process drifting between two response boundaries. When the process reached the upper boundary (denoted as 1), the gamble was to be accepted and when the process reached the bottom boundary (denoted as 0), the gamble was to be rejected. The starting point of the process was denoted by z. The velocity of the drift process, or drift rate, was defined as $v = v_G \cdot G - v_L \cdot L + b + \varepsilon$, where G and L denoted the magnitudes of potential gain and loss, v_G and v_L denoted the respective weights, b denoted an intercept, and ε denoted random noise that followed a standard normal distribution. In addition, non-decision time (t) and boundary separation (a) were also included as variables of non-interests. The current study focused on the decomposition of electrophysiological signatures for response bias (0.5-z) and valuation bias [ln (v_L / v_G)] that were dissociated in our earlier work.[28] The main results of other parameters in our model were reported in Figure S7.

In addition to the main model, we also tested three reduced models that constrained valuation bias (DDM3, set v_G=v_L), response bias (DDM2, set z=0.5) or both biases (DDM1), and an extended model that incorporated P3 as an additional additive variable in the drift rate (DDM5). All of the five models were fit to choices and response times using the Python toolbox HDDM.[89] However, estimation was performed for each subject individually to avoid endogenous correlation in hierarchical estimation. For each model, we drew 6,000 posterior samples with the first 2,000 discarded as burn-in.

Prospect theory model

Following our earlier work,[28] the expected utility of accepting a gamble (U_A) was modeled as the sum of probability-weighted gain (G) and loss (L), i.e., $U_A = 0.5 \cdot G - 0.5 \cdot \lambda \cdot L$, where λ indicated the weight of loss relative to gain. The expected utility to reject a gamble was assumed to be zero, i.e., $U_R = 0$. The probability of accepting a gamble (P_A) was computed by the softmax function, $P_A = 1/\{1+\exp[-\mu(U_A - U_R)]\}$, where μ indicated the degree to which a decision was sensitive to expected utility. The probability of rejecting a gamble was calculated as $P_A = 1 - P_R$. Maximum likelihood estimation was then employed to identify the values of λ and μ. PT loss aversion was quantified as the log-transformed weight of loss, i.e., ln (λ), which was thereby comparable with DDM valuation bias [ln (v_L / v_G)].

T-tests and regression analyses

All t-tests were two-tailed. For regression analyses, all regressors were rescaled between 0 and 1. For multilevel-regressions, random effects of participants were included for the intercept and all regressors. Comparisons of coefficients between each pair of regressors were conducted using *linhyptest* function in MATLAB.